Synthesis of conductive polymeric nanoparticles with hyaluronic acid based bioactive stabilizers for biomedical applications

Materials Today Chemistry 25 (2022) 100969

Contents lists available at ScienceDirect

Materials Today Chemistry

journal homepage: www.journals.elsevier.com/materials-today-chemistry/

Synthesis of conductive polymeric nanoparticles with hyaluronic acid based bioactive stabilizers for biomedical applications

C. Winters [a], F. Zamboni [a, b], A. Beaucamp [a], M. Culebras [d], M.N. Collins [a, b, c, *]

[a] Stokes Labs, Bernal Institute, School of Engineering, University of Limerick, Ireland
[b] Health Research Institute, University of Limerick, Ireland
[c] SFI AMBER Centre, University of Limerick, Ireland
[d] Institute of Material Science, University of Valencia, Spain

A R T I C L E I N F O

Article history:
Received 19 January 2022
Received in revised form
6 April 2022
Accepted 25 April 2022
Available online xxx

Keywords:
PEDOT:PSS
Electrical conduction
Biocompatibility
Tissue scaffolds

A B S T R A C T

In recent years, the use of organic materials to infer conductivity in biomedical devices has received increasing attention. Typical inorganic semiconductors and conductors are rigid and expensive, usually require multiple processing steps and are unsuitable for biomedical applications. Electrochemically or chemically doped conjugated polymers help to overcome these problems due to their stability, low cost, light weight and excellent electrical and optical properties. The conducting polymer poly(3,4-ethylenedioxythiophene): polystyrene sulfonate (PEDOT:PSS) is the material of choice for biomedical applications as it is water soluble, however, there are growing concerns around its stabilizer, PSS, due to its release of acidic products upon degradation *in-vivo*. Here, we report the successful synthesis of PEDOT nanoparticles using hyaluronic acid (HA) as a stabilizer via an oxidative miniemulsion polymerisation technique. This improves the bioactivity and hydrophilicity of nanoparticles. The effect of varying amounts of HA and different molar ratios of EDOT:TOS has been studied and their role in the conductive and morphological properties of final nanoparticles has been fully elucidated. Furthermore, bioactivity and biocompatibility of the nanoparticles are demonstrated for customizable *in vivo* applications. Nanoparticles were found to have a conductivity up to 10 times greater than pristine PEDOT:PSS with increased addition of oxidant. The proposed easy-to-manufacture approach, along with the highlighted superior properties, expands the potential of conductive polymers in future customizable biological applications such as tissue scaffolds, nerve conduits and cardiac patches and represents a real breakthrough from the current state of the art.

1. Introduction

Nanomaterials are ubiquitous with their ability to be tailored for use in multiple areas related to biomedical engineering and health such as drug delivery, biosensors, antimicrobial applications, cancer therapy and tissue engineering [1–4]. Intrinsically conductive polymeric (ICP) nanoparticles are organic materials which possess the combined properties of a semiconductor or metal and those of a conventional polymer. They possess a semiconductor's electrical, optical and magnetic properties with low cost, biocompatibility and corrosion resistance [5] rendering them ideal for biomedical applications. They combine ionic and electronic conductivity allowing effective transfer of electrical signals at cell interfaces [6]. One common conducting polymer is poly(3,4-ethylenedioxythiophene) (PEDOT) which is synthesised using a stabilizer PSS (polystyrene sulfonate). PEDOT has many desirable characteristics such as facile processing, high conductivity and commercial availability. It has been widely deployed in the emerging area of organic electronics in applications such as organic light-emitting diodes (OLEDs) [7–10]. However, there are limitations associated with PEDOT:PSS in biological applications, as excess PSS negatively affects conductivity, long-term stability, specific capacity and crucial biocompatibility. There are also concerns regarding PSS degradation and the potential release of harmful acidic components *in-vivo* [11,12]. Previous studies have investigated alternatives for PSS such as a study by del Agua et al. in which scaffolds based on PEDOT: xanthan gum were found to have tuneable porosity and mechanical properties. These scaffolds combine both the traditional conductivity of PEDOT and additional biocompatibility and mechanical qualities of xanthan gum, showing some promise as an alternative to PEDOT:PSS [13].

* Corresponding author.
E-mail address: maurice.collins@ul.ie (M.N. Collins).

https://doi.org/10.1016/j.mtchem.2022.100969

Conductive polymers may be synthesized electrochemically, via chemical oxidation or photoelectrochemically [14–16]. An important structural factor in chemical synthesis is solubility, as in order to reach a suitable molecular weight, low molecular weight polymers and oligomers must be soluble enough to be able to polymerize and become stable. ICPs are generally insoluble in water. In order to be incorporated into biological systems or in hydrogels solubility is desirable and advantageous as it acts as a hydrophilic nanocapsule for the hydrophobic monomer. In conjunction with a suitable oxidant such as FeTos, the selective generation of cation radicals at a desired location on the monomer, is possible for efficient oxidation [17].

In the biomedical device industry, naturally occurring biomaterials are of enormous interest due to their inherent biocompatibility, bioactivity and biodegradability *in vivo* [18,19]. Hyaluronic acid (HA) is found naturally in the tissue's extracellular matrix (ECM) and is necessary for functions within the body such as regulating cell differentiation and migration, immune modulation, and wound healing [20]. It is also being studied for applications including wound dressings and antibacterial hydrogels [21], cell encapsulation [22,23], scaffolds for tissue engineering [22,24–26], drug delivery [27] and hydrogels [28]. For this reason, it has become the material of choice for body repair. The use of HA in the synthesis of PEDOT nanoparticles has previously been completed by Wang et al. in which HA-doped nanoparticles were synthesized using chemical oxidative polymerization techniques. These nanoparticles were then synthesized into PLLA films and showed good neurite outgrowth upon electrical stimulation, proving to be a promising candidate for nerve regeneration in tissue engineering applications [29].

This work herein describes, for the first time, the synthesis of conductive and biocompatible PEDOT nanoparticles using bioactive HA as a stabilizer via oxidative miniemulsion polymerization. This study shows a complete analysis of the synthesized particles using biological, electrical, morphological and chemical analysis. The dopant used is TOS, therefore we use the nomenclature of PEDOT:TOS. Uniquely, HA is used as a stabilizer of the EDOT droplets during the miniemulsion processes and this is of importance because HA is located on the surface of the PEDOT NPs. This allows further surface functionalization for possible future cell therapies or electrically stimulated drug delivery. We further envisage their deployment dispersed within hydrogels and scaffolds for application as cardiac patches, nerve conduits and in the regeneration of various electrically conducting tissues.

2. Experimental section

2.1. Materials

3,4 Ethylenedioxythiophene (EDOT, 97%), iron(III) p-toluenesulfonate hexahydrate (FeTos), hydrochloric acid and poly(3,4-ethylenedioxythiophene) polystyrene sulfonate (PEDOT:PSS) (1.3 wt%) were purchased from Sigma Aldrich (Ireland), sodium hyaluronic acid (HA, 23.2 kDa) was purchased from Shanghai Easier Industrial Development Co. Ltd. (Shanghai, China), hydrogen peroxide 30 wt% was supplied by Analab Ltd. For cell culture experiments, Dulbecco's modified minimal essential medium (DMEM), penicillin-streptomycin, L-glutamine, calcein AM and propidium iodine were purchased from Sigma Aldrich (Ireland). alamarBlue was purchased from Thermofisher Ireland.

2.2. Synthesis of PEDOT:TOS nanoparticles

Varied amounts of HA were dissolved in 40 mL of hydrochloric acid (HCl) solution (0.1 M). EDOT (0.2 mL, 1.8×10^{-3} mol) was added to this solution and stirred for 10 min. The mixture is placed in an ice bath under tip ultrasonication with a Branson Sonifier 450 (1/2 inch tip, amplitude of 70%, pulse of 90%) for 10 min to form a miniemulsion, as shown in Fig. 1A. Meanwhile, a FeTos solution was prepared in 10 mL of deionized (DI) water, see Table 1, and stirred for 10 min. The resulting milky emulsion is placed under sonification and added to a reaction flask under further stirring. The FeTos solution was added dropwise to the reaction flask and the mixture was left to initiate polymerization. After 1 h, 0.05 mL of hydrogen peroxide (7.5×10^{-3} mol) was added, and the solution was left to polymerize overnight. The change in color profile of the miniemulsion upon addition of FeTos and H_2O_2 can be tracked in Fig. 1B.

Nanoparticles were purified via centrifugation at 8000 rpm for 10 min, three times, redispersing in DI water after each run. After the third run, with excess FeTos removed, a transparent color was observed in the solution. Following this, nanoparticles were redispersed in 40 mL of DI water and sonicated for 20 min in a sonication bath.

2.3. Characterization

A glass slide was covered in NP solution and dried overnight to evaporate water, leaving a film of nanoparticles. The morphological characteristics of the nanoparticles were characterized using a Hitachi SU-70 Scanning electron microscope (SEM) at an accelerating voltage of 5 kV at a working distance of 14 mm. Prior to analysis, samples were placed in a sample holder and coated with a thin layer of gold.

UV–vis spectroscopy was performed using a Shimadzu UV-1800 spectrophotometer in the range of 1100 nm–200 nm. Samples were diluted in order to allow for sufficient light to pass through the solutions and the resulting graphs were normalized.

Raman spectroscopy was performed using a Horiba, LabRAM 1A Raman spectrometer in backscattering configuration, equipped with a 532 nm laser. The filter was set to 0.1% to avoid degradation of the sample, the hole of aperture was 200 μm and the silt was set to 100 μm for all spectra readings. The spectra were captured from 1250 to 1700 cm^{-1}, with 120 s exposure time and five acquisitions for each reading. In order to avoid inaccuracy, the spectrometer was calibrated with the spectra of a silicon sample beforehand.

In order to test the conductivity of the nanoparticles a film of each formulation was produced, similarly to the method above, with an undiluted initial solution. To determine the conductivity of the films the Van der Pauw method was used:

$$e^{-\pi d R_1 \sigma} + e^{-\pi d R_2 \sigma} \tag{1}$$

where d is the film thickness, R_1 and R_2 are the resistance in direction 1 and 2 respectively and σ is the electrical conductivity of the film.

Four points of silver paint were painted on the surface of the film, with four contact points used in order to reduce the effect of contact resistance. A Keithley 2400 SourceMeter was utilized to produce a current through the sample and the resistance was measured.

For biocompatibility testing, solutions in their liquid suspension form were sterilized by using autoclave and by UV sterilization. Three concentrations of each formulation were used (0.5 mL, 0.05 mL and 0.005 mL). NIH/3T3 fibroblast cells were grown in DMEM supplemented with 10% foetal bovine serum (FBS), 1% glutamine and 1% streptomycin-penicillin in a 5% CO_2 environment. Cells were seeded with the pre-conditioned PEDOT:TOS nanoparticle solutions at a density of 50×10^3 cells/well in a 24-well plate and 1 mL of cell culture media in each well and incubated for 4 h. A control was also prepared that consisted of 1 mL of media with the same density of cells.

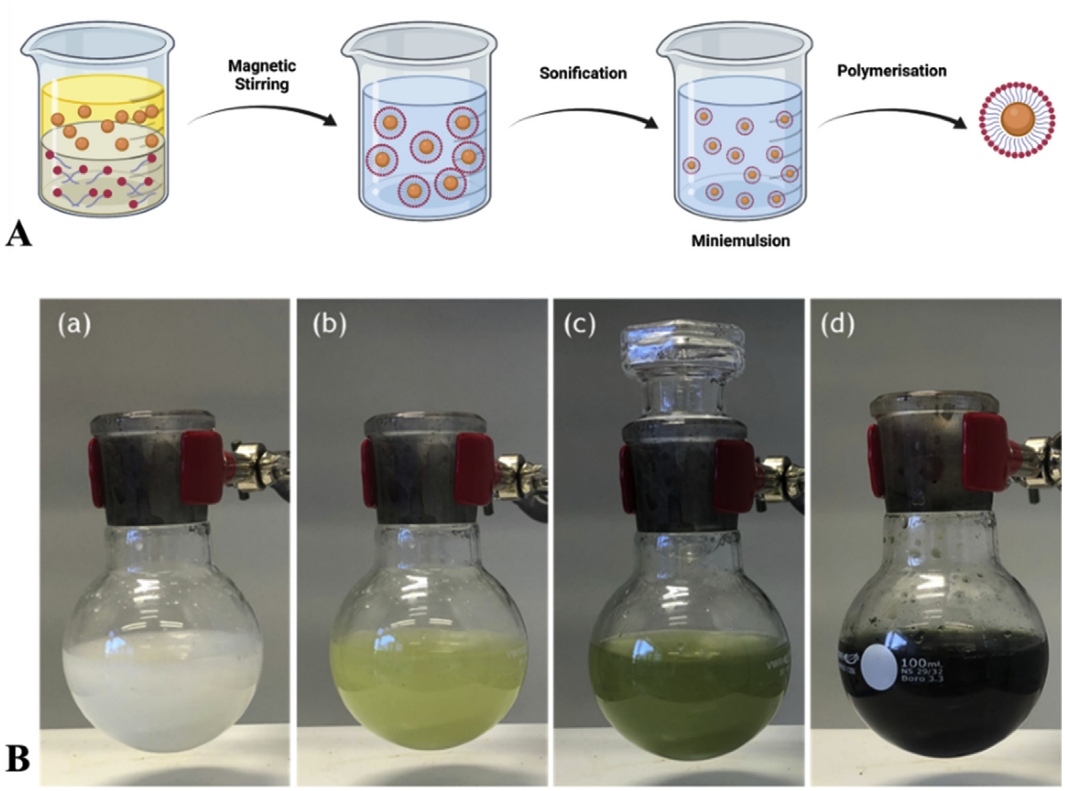

Fig. 1. (A): Process of Miniemulsion Polymerization; (B): Color change of the solution during synthesis (a) Miniemulsion solution following sonication, (b) Solution following the addition of 2 mL oxidant, (c) Solution following addition of 10 mL of oxidant, (d) Solution following addition of H_2O_2.

Table 1
Formulations using varied amounts of HA and FeTos.

Formulation	Molar ratio EDOT:TOS	Hyaluronic acid (wt%)	Hyaluronic acid (M)	EDOT (mL)	FeTos (g)	FeTos (M in H_2O)	H_2O_2 (mL)
EDOT:TOS1:0.5 HA0.2%	1:0.5	0.2	1.78×10^{-4}	0.2	0.6385	1.4×10^{-2}	0.05
EDOT:TOS1:0.5 HA0.5%	1:0.5	0.5	4.45×10^{-4}	0.2	0.6385	1.4×10^{-2}	0.05
EDOT:TOS1:0.5 HA0.7%	1:0.5	0.7	6.23×10^{-4}	0.2	0.6385	1.4×10^{-2}	0.05
EDOT:TOS1:0.5 HA1%	1:0.5	1	8.9×10^{-4}	0.2	0.6385	1.4×10^{-2}	0.05
EDOT:TOS1:1 HA0.2%	1:1	0.2	1.78×10^{-4}	0.2	1.277	2.8×10^{-2}	0.05
EDOT:TOS1:1 HA0.5%	1:1	0.5	4.45×10^{-4}	0.2	1.277	2.8×10^{-2}	0.05
EDOT:TOS1:1 HA0.7%	1:1	0.7	6.23×10^{-4}	0.2	1.277	2.8×10^{-2}	0.05
EDOT:TOS1:1 HA1%	1:1	1	8.9×10^{-4}	0.2	1.277	2.8×10^{-2}	0.05
EDOT:TOS1:2 HA0.2%	1:2	0.2	1.78×10^{-4}	0.2	2.554	5.6×10^{-2}	0.05
EDOT:TOS1:2 HA0.5%	1:2	0.5	4.45×10^{-4}	0.2	2.554	5.6×10^{-2}	0.05
EDOT:TOS1:2 HA0.7%	1:2	0.7	6.23×10^{-4}	0.2	2.554	5.6×10^{-2}	0.05
EDOT:TOS1:2 HA1%	1:2	1	8.9×10^{-4}	0.2	2.554	5.6×10^{-2}	0.05

To evaluate the cell cytotoxicity, alamarBlue reagent was added to each sample at a concentration of 10% as specified by the manufacturer. The well plates were re-incubated and the samples were taken at 30 min, 24 h and 48 h in 96 well-plates with fluorescence measured at 540 and 590 nm using a SynergyMx plate reader (BioTek, EUA). Pre-conditioned PEDOT:TOS samples, PEDOT:PSS samples and NIH/3T3 fibroblast cells were then assessed for cell viability and adhesion. The cells were stained with calcein AM and propidium iodine for fluorescence imaging and visualized using the Zeiss LSM 710 Confocal Microscope.

Parametric data obtained from the cell cytotoxicity tests were analyzed using one-way ANOVA test using R software program, with the *p*-value of <0.05 considered as statistically significant.

3. Results and discussion

3.1. Oxidative miniemulsion polymerisation

PEDOT:TOS nanoparticles were synthesized by oxidative miniemulsion polymerization, using HA as a stabilizer and FeTos as an oxidant. Initially, the monomer solution and the oxidant solution were prepared using deionized water. However, in this case when the oxidant solution was added to the monomer solution, the nanoparticles tended to agglomerate. This was attributed to a pH mismatch between the two steps, the pH of the PEODT and FeTos solutions being an acidic 1–2 and the hyaluronic acid having a neutral pH of 6–7. Accordingly, the oxidant solution was dissolved in 0.1 M of HCl to reach a similar pH to that of the monomer solution and thereby more stable particle dispersions were obtained. This was the method used for all the formulations detailed in Table 1. Solutions remained stable for a number of weeks before they began to agglomerate, however redispersion is easily achieved upon sonification. H_2O_2 is needed in the synthesis in order to regenerate Fe^{3+} ions that are reduced to Fe^{2+} ions during oxidative polymerization, this allows the further polymerization of EDOT to take place. Addition of H_2O_2 also increased solution stability with an immediate color change to dark blue/ black upon its addition.

3.2. Morphological analysis

In Fig. 2, at a low percentage of HA, crystallites can be seen but as the percentage of HA increases, these crystal-like structures disappear with more agglomeration occurring, making it difficult to identify individual particles. In Figure A in the supplementary documentation, crystals can be seen, these crystals are likely to be formed from the addition of hydrogen chloride, as the oxidant is removed following formulation in the form of chloride salt crystals. Fig. 2 shows an increase in aggregation with an increase in the molar ratio of EDOT:TOS with the 1:2 ratio showing flaky type films as opposed to the other samples that tend to form a smoother surface. This indicates that for films, a ratio of 1:1 or 1:0.5 is best.

The nanoparticle size was observed from SEM micrographs in Fig. 2 with a range from 52 to 90 nm and an average size of 71 nm. The morphology of the nanoparticles is not as rounded or defined as seen in the synthesis of PEDOT:PSS nanoparticles via mini-emulsion polymerization [30]. This may be due to the use of hyaluronic acid as a stabilizer and the distinct difference in pH it creates in the synthesis process. The use of hydrochloric acid to improve this disparity works well to improve the stability of the final formulations but influences the final morphology of the nanoparticles and the formation of chloride salt crystals, as seen in the supporting documentation.

3.3. Doping of nanoparticles

In order to study the degree of doping of the nanoparticles, Raman and UV−vis spectroscopy were used. The UV−vis spectra of the various concentrations of HA with varied ratios of FeTos can be seen in Fig. 3. The spectra show a trend typical of PEDOT. The absorption of oxidized states can be observed in all spectra, and this

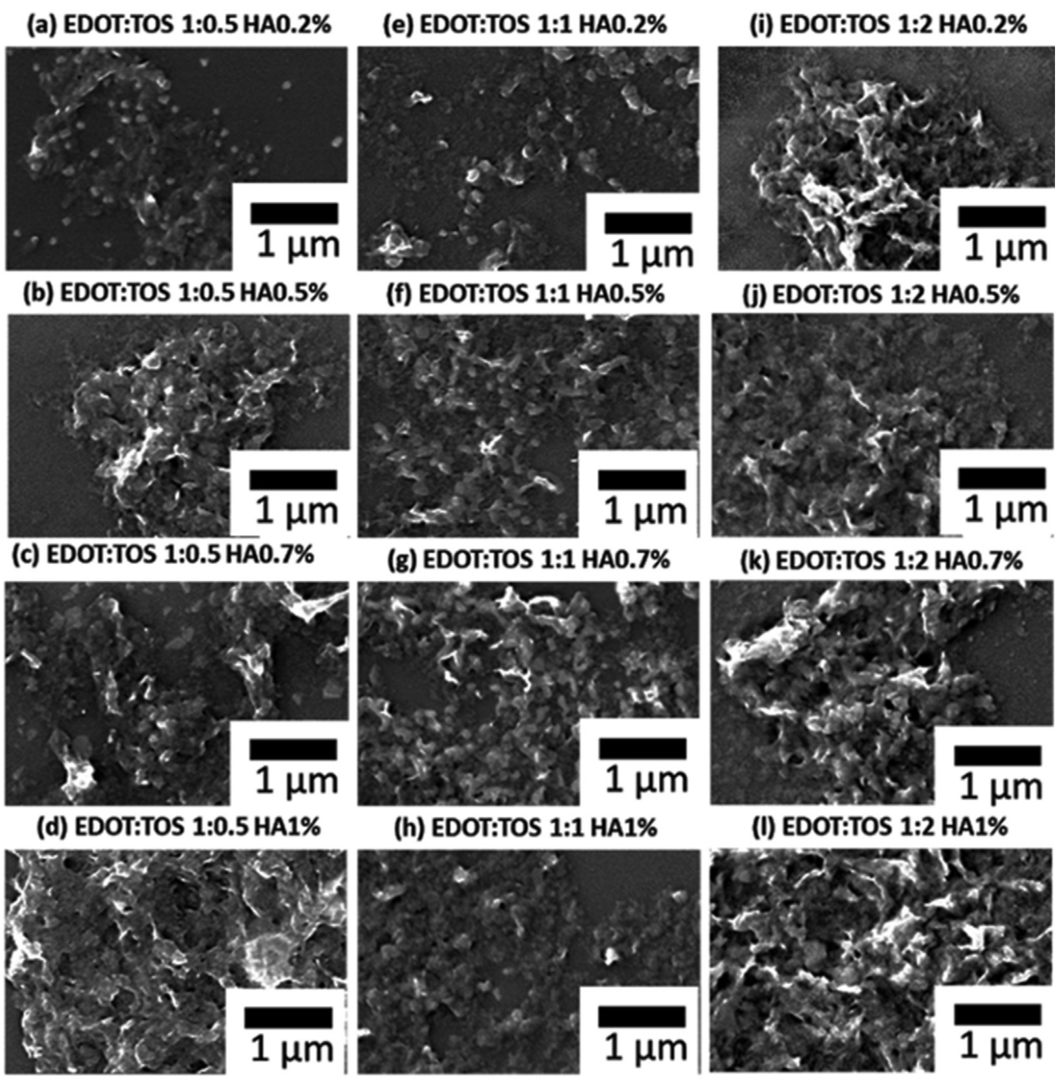

Fig. 2. SEM images of all nanoparticles. (a−d) EDOT:TOS 1:0.5, HA 0.2%, 0.5%, 0.7%, 1% respectively. (e−h) EDOT:TOS 1:1, HA 0.2%, 0.5%, 0.7%, 1% respectively. (i−l) EDOT:TOS 1:2, HA 0.2%, 0.5%, 0.7%, 1% respectively.

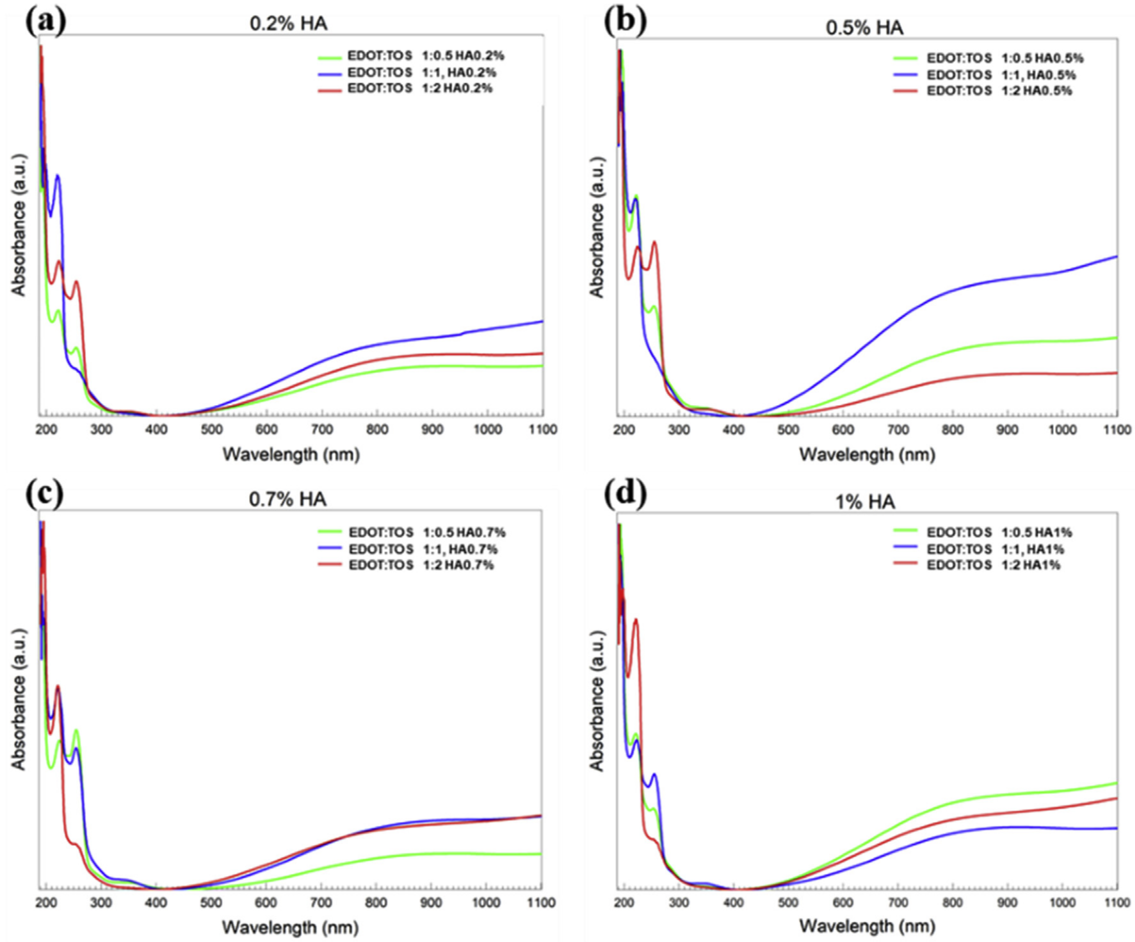

Fig. 3. UV–vis spectra of samples with HA percentage of (a) 0.2%, (b) 0.5%, (c) 0.7% and (d) 1%.

indicates that there is high oxidation within the polymer chains. The polaronic and bipolaronic region are seen from 800 to 1000 nm and the absorption related to these states can be seen to generally increase with a higher concentration of FeTos with EDOT:TOS 1:1 and 1:2 showing higher absorptions than 1:0.5 on average due to higher doping in these formulations. The absorption that relates to the neutral π-bonds is low in all samples. This is possibly due to the addition of H_2O_2, as the OH radicals from the H_2O_2 interact with the radicals generated from the neutral π system during polymerization. This results in the breaking of the conjugation in the PEDOT chain as the OH radicals bond to the polymer backbone. This is associated with a decrease in conductivity, as the electrical charges cannot propagate as efficiently along the polymer chains. The bonding of hydroxyl groups to the polymer backbone as a result of the addition of H_2O_2 is postulated by these results.

For Raman spectroscopy, the filter was set to 0.1% and the typical vibrational modes for PEDOT are seen within the range of 1250 and 1700 cm^{-1}

Fig. 4 compares the spectra at each percentage of HA. A low Raman signal was observed at the lowest FeTos concentration (EDOT:TOS 1:0.5) and this signifies a low degree of polymerization in these samples. In general, the maximum Raman signal can be seen in the EDOT:TOS 1:1 samples and this signifies a low doping level in PEDOT and thus, an increase in the number of neutral π-bonds in the polymer backbone. However, a higher absorption is seen with a higher doping level in the EDOT:TOS 1:2 final samples and thus the Raman signal decreases. The reason for a decrease in intensity is due to asymmetric stretching of the C═C bonds in the doped state as well as a decrease in the number of neutral π-bonds along the polymer backbone.

3.4. Electrical characterization

Electrical conductivity of the NPs was measured using the Van der Pauw method, as described in Section 2.3. Fig. 5 shows the conductivity of each sample as a function of the molar ratio of EDOT:TOS used to prepare the formulations. As expected, there is a general increase in conductivity with an increase in FeTos. The films of ratio 1:0.5 EDOT:TOS have an average conductivity of 14.02 S/cm, the films of ratio 1:1 are seen to have a slightly higher average conductivity of 16.9 S/cm. However, there is a significant increase in the conductivity seen at the ratio 1:2 EDOT:TOS as it rises to an average of 30.3 S/cm, this is much higher than lower ratios as the oxidation levels of PEDOT is higher with an increase in EDOT:TOS molar ratio. Another possible reason for this increased conductivity at a higher oxidant level is the tendency for these nanoparticles to agglomerate more with increased oxidant. Higher agglomeration would mean that the nanoparticles would be more interconnected, meaning the charge would pass through the film more easily for an EDOT:TOS ratio of 1:2 than for 1:1 or 1:0.5.

Pristine PEDOT:PSS films prepared in the lab yielded a conductivity of 0.5–5.1 S/cm. The conductivity results found in this study are similar to that of the conductivity seen in other studies using pristine PEDOT:PSS nanoparticle films in which a conductivity of 0.1–10 S/cm can be seen [31–33]. In order to improve its

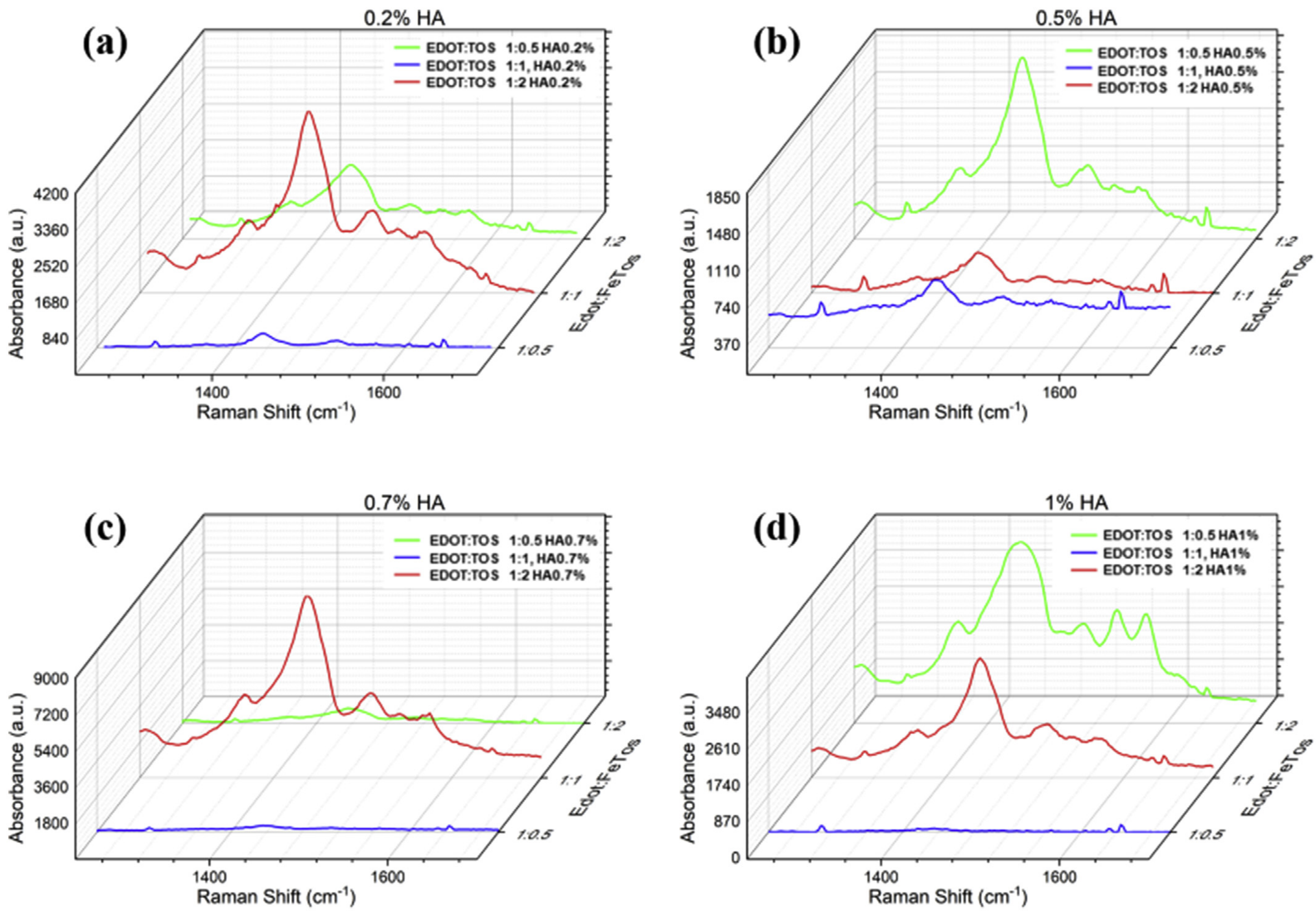

Fig. 4. Raman spectra of (a) 0.2% HA, (b) 0.5% HA, (c) 0.7% HA and (d) 1% HA.

conductivity, pristine PEDOT:PSS has been treated with organic solutions to achieve a conductivity of up to 2100 S/cm [34] or with hydrothermal treatments [35]. Without treatment however, PEDOT:TOS films show improved conductivity to that of pristine PEDOT:PSS films. This is promising for the potential use of hyaluronic acid as a natural alternative to other synthetic stabilizers in conductive applications. In order to back up this finding, the biocompatibility of the nanoparticles was examined using biocompatibility testing.

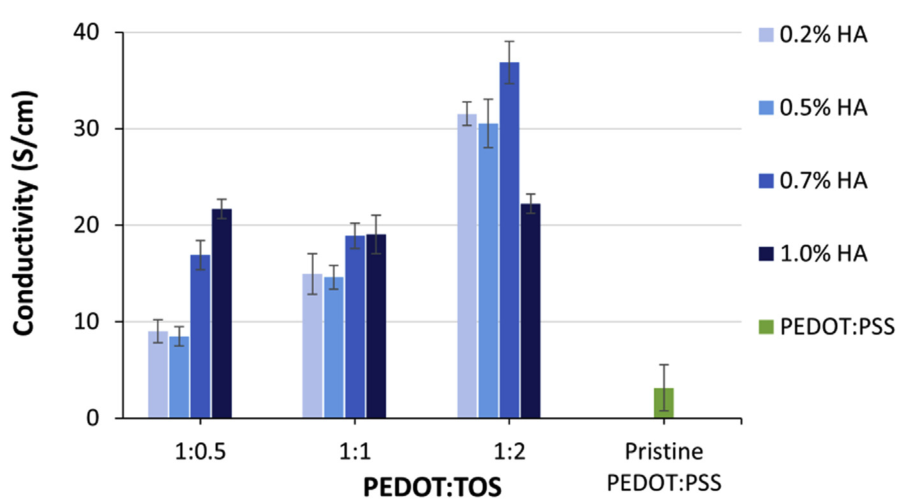

Fig. 5. The conductivity of PEDOT:TOS and PEDOT:PSS films using the Van der Pauw equation.

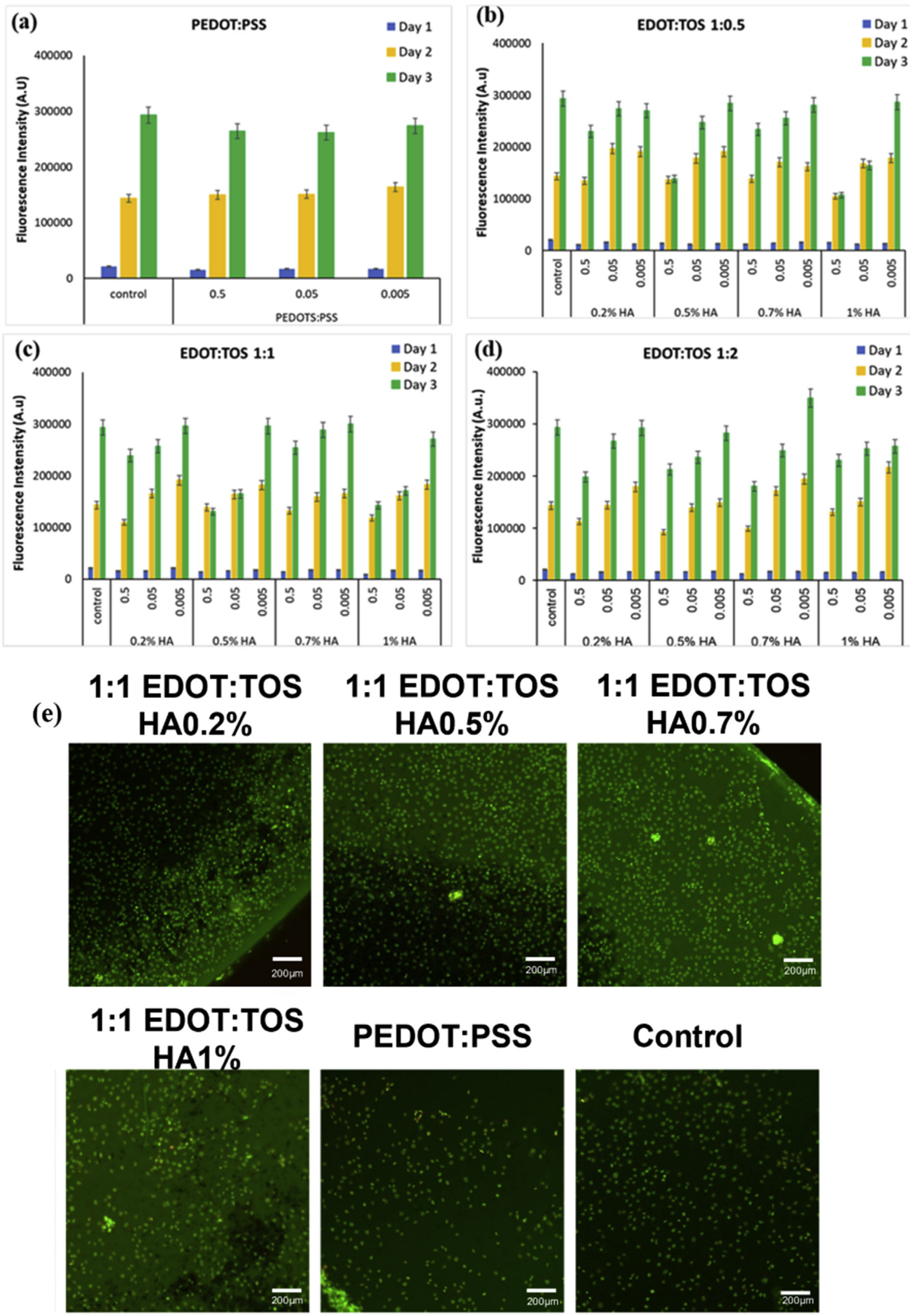

Fig. 6. Fluorescence of samples over three days: (a) PEDOT:PSS, (b) EDOT:TOS 1:0.5, (c) EDOT:TOS 1:1, (d) EDOT:TOS 1:2. (e) LIVE-DEAD assay. For all tests NIH/3T3 fibroblast cells were cultured in the presence of the PEDOT:TOS/PEDOT:PSS nanoparticles over a period of 96 h. Magnification 4×.

3.5. Biocompatibility characterisation

The biocompatibility of the nanoparticles is shown in Fig. 6. Nanoparticle formulations show a similar proliferation profile to that of the control. Generally, the lowest ratio of 0.005% of all samples shows the highest proliferation which is to be expected as that is the solution that most resembles the control with the lowest amount of nanoparticles.

However, all solutions show a continued increase in fluorescence over the three days which indicates that they have good cell biocompatibility over time. This is important for possible future *in vivo* applications as the NPs and their degradation products would need to have a sustained biocompatibility for a prolonged period. These results are promising for increased bioactivity in PEDOT nanoparticles and as HA degradation is well known, it will not cause any detrimental side-effects *in vivo* [36,37]. This is supported by the *p*-values calculated from the ANOVA, see Table A found in the supplementary documentation, with a statistical difference found in each of the groups with regards to the increase in fluorescence over the three days.

Fluorescent images of the cells cultured with PEDOT:TOS, 1:1 EDOT:TOS nanoparticles were captured using a confocal microscope and presented in Fig. 6(e), where dead cells are stained red and live cells are stained green. Very few dead cells were observed in all nanoparticle groups, with mostly live cells present. The cells in the PEDOT:TOS nanoparticle groups were similar in morphology to the cells in the control and PEDOT:PSS groups. Cells were also seen to be accumulating towards the edges of the well plates in the PEDOT:TOS groups which is likely to be due to the agglomeration of these nanoparticles over time as this is not seen in the PEDOT:PSS and control groups.

Interestingly, the PEDOT:PSS nanoparticles characterized in this study showed similar fluorescence and cell viability to that of both the control and the synthesized PEDOT:TOS nanoparticles. This is unusual compared to that of other biocompatibility studies conducted on PEDOT:PSS in which they are found to be cytotoxic, sample data can be found in figure C in the supplementary documentation. This is probably due to the low concentration used of the liquid PEDOT:PSS as the results shown in figure C from biocompatibility studies done with mesenchymal stem cells show much lower levels of fluorescence and proliferation. In the studies shown in figure C the PEDOT:PSS is used in its original dilution as well as in a dilution factor of 1:3 as opposed to the dilution of 0.5%, 0.05% and 0.005% used in this study. As PEDOT:PSS is a liquid and the formulations produced are nanoparticle dispersions, the dilution factor used may not be fully comparable due to their differences in formulation. This indicates that PEDOT:PSS should have a higher cytotoxicity when used in its usual, more diluted form and that these results are not as indicative to its biocompatibility than other studies.

This data suggests that the use of hyaluronic acid as stabilizer does not show any cytotoxic effect on cultured fibroblast cells and thus suggests that these nanoparticles are biocompatible. These results do not show any significant disparity between these nanoparticles compared to control or PEDOT:PSS groups. The ratio of hyaluronic acid does not seem to have an effect on the viability of NIH/3T3 cells, but increased amounts do show increased accumulation of cells at the edges of dishes which could be due to increased agglomeration of the nanoparticles at higher ratios of HA. As these nanoparticles have the potential for use within scaffold materials, these findings indicate that lower concentrations of nanoparticles may benefit uniform distribution within the scaffold and allow better bioactivity in future applications.

4. Conclusions

Stable, conducting and biocompatible PEDOT:TOS nanoparticles were successfully synthesized via oxidative miniemulsion polymerization. Conductivity reached up to 37 S/cm through these nanoparticle films compared to 0.5–5.1 S/cm for pristine PEDOT:PSS films. The ratio of oxidant added influenced the conductivity of the nanoparticles, with an increase in the EDOT:TOS ratio leading to an increase in conductivity due to increased oxidation. The morphology of the nanoparticles was also affected by increased oxidant, with higher ratios showing agglomerated, flaky films and low ratios showing well-defined nanoparticles. The nanoparticles also show good biocompatibility over a 3-day biocompatibility test, with increased fluorescence similar to that of a control and very low numbers of dead cells observed during live/dead analysis. Agglomeration did occur however in higher ratios of HA and oxidant and thus this agglomeration would have to be reduced for incorporation into biological scaffolds. Overall, characterization showed good promise for the use of hyaluronic acid as an alternative to the cytotoxic PSS as a stabilizer for PEDOT. From these findings it can be concluded that the synthesized hyaluronic acid stabilized PEDOT nanoparticles show good potential for conductive and biological applications. These nanoparticles show good promise for the future development of natural conducting polymers for the regeneration of tissues and drug delivery.

CRediT author statement

Caitriona Winters: Data curation, Formal analysis, Investigation, Writing - Original Draft. **Fernanda Zamboni:** Data curation, Methodology, Formal analysis, Investigation, Writing - Original Draft. **Anne Beaucamp:** Data curation, Formal analysis, Writing - Original Draft, Supervision. **Mario Culebras:** Validation, Investigation, Formal analysis, Writing – original draft. **Maurice N Collins:** Conceptualization, Methodology, Formal analysis, Supervision, Resources, Writing - Review & Editing.

Data availability

The raw/processed data required to reproduce the above findings cannot be shared at this time as the data also forms part of an ongoing study.

Declaration of competing interest

The authors declare that they have no known competing financial interests or personal relationships that could have appeared to influence the work reported in this paper.

Acknowledgements

MNC would like to thank the School of Engineering at the University of Limerick for supporting this work.

Appendix A. Supplementary data

Supplementary data to this article can be found online at https://doi.org/10.1016/j.mtchem.2022.100969.

References

[1] M. Mabrouk, D.B. Das, Z.A. Salem, H.H. Beherei, Nanomaterials for biomedical applications: production, characterisations, recent trends and difficulties, Molecules 26 (4) (2021) 1077.

[2] J.K. Patra, et al., Nano based drug delivery systems: recent developments and future prospects, J. Nanobiotechnol. 16 (1) (2018) 71, 2018/09/19. https://doi.org/10.1186/s12951-018-0392-8.

[3] A. Hasan, M. Morshed, A. Memic, S. Hassan, T.J. Webster, H.E.-S. Marei, Nanoparticles in tissue engineering: applications, challenges and prospects (in eng), Int. J. Nanomed. 13 (2018) 5637–5655, https://doi.org/10.2147/IJN.S153758.

[4] J. Hasan, Y. Xu, T. Yarlagadda, M. Schuetz, K. Spann, P.K.D.V. Yarlagadda, Antiviral and antibacterial nanostructured surfaces with excellent mechanical properties for hospital applications, ACS Biomater. Sci. Eng. 6 (6) (2020) 3608–3618, 2020/06/08. https://doi.org/10.1021/acsbiomaterials.0c00348.

[5] S. Tajik, et al., Recent developments in conducting polymers: applications for electrochemistry, RSC Adv. 10 (62) (2020) 37834–37856, https://doi.org/10.1039/D0RA06160C.

[6] B.D. Paulsen, K. Tybrandt, E. Stavrinidou, J. Rivnay, Organic mixed ionic–electronic conductors, Nat. Mater. 19 (1) (2020) 13–26, https://doi.org/10.1038/s41563-019-0435-z, 2020/01/01.

[7] G.-F. Wang, X.-M. Tao, R.-X. Wang, Fabrication and characterization of OLEDs using PEDOT:PSS and MWCNT nanocomposites, Compos. Sci. Technol. 68 (14) (2008) 2837–2841, https://doi.org/10.1016/j.compscitech.2007.11.004, 2008/11/01/.

[8] D.G. Yoon, M. Kang, J.B. Kim, K.-T. Kang, Nozzle printed-PEDOT:PSS for organic light emitting diodes with various dilution rates of ethanol, Appl. Sci. 8 (2) (2018), https://doi.org/10.3390/app8020203.

[9] D.T. Simon, E.O. Gabrielsson, K. Tybrandt, M. Berggren, Organic bioelectronics: bridging the signaling gap between biology and technology, Chem. Rev. 116 (21) (2016) 13009–13041, https://doi.org/10.1021/acs.chemrev.6b00146, 2016/11/09.

[10] D. Mantione, I. Del Agua, A. Sanchez-Sanchez, D. Mecerreyes, Poly(3,4-ethylenedioxythiophene) (PEDOT) derivatives: innovative conductive polymers for bioelectronics (in eng), Polymers (Basel) 9 (8) (Aug 2017), https://doi.org/10.3390/polym9080354.

[11] M. Asplund, H. von Holst, O. Inganäs, Composite biomolecule/PEDOT materials for neural electrodes (in eng), Biointerphases 3 (3) (Sep 2008) 83–93, https://doi.org/10.1116/1.2998407.

[12] D. Mantione, et al., Poly(3,4-ethylenedioxythiophene):GlycosAminoGlycan aqueous dispersions: toward electrically conductive bioactive materials for neural interfaces, Macromol. Biosci. 16 (8) (2016) 1227–1238, https://doi.org/10.1002/mabi.201600059, 2016/08/01.

[13] I. del Agua, et al., Conducting polymer scaffolds based on poly(3,4-ethylenedioxythiophene) and xanthan gum for live-cell monitoring, ACS Omega 3 (7) (2018) 7424–7431, https://doi.org/10.1021/acsomega.8b00458, 2018/07/31.

[14] A. Watoni, I. Noviandri, M. Nurdin, L.O.A. Ramadhan, Electrocoating polypyrrole on gold-wire electrode as potential mediator membrane candidate for anionic surfactant electrode sensor, J. Kimia Sains dan Aplikasi 23 (05/31 2020) 167–176, https://doi.org/10.14710/jksa.23.5.167-176.

[15] A. Dominguez-Alfaro, et al., 3D printable conducting and biocompatible PEDOT-graft-PLA copolymers by direct ink writing, Macromol. Rapid Commun. 42 (12) (2021) 2100100, https://doi.org/10.1002/marc.202100100, 2021/06/01.

[16] G. Samu, C. Visy, K. Rajeshwar, S. Sarker, V. Subramanian, C. Janáky, Photoelectrochemical infiltration of a conducting polymer (PEDOT) into metal-chalcogenide decorated TiO2 nanotube Arrays, Electrochim. Acta 151 (01/01 2015) 467–476, https://doi.org/10.1016/j.electacta.2014.11.094.

[17] K. Landfester, Miniemulsion polymerization and the structure of polymer and hybrid nanoparticles, Angew. Chem. Int. Ed. 48 (25) (2009) 4488–4507, https://doi.org/10.1002/anie.200900723.

[18] M.S. Reddy, D. Ponnamma, R. Choudhary, K.K. Sadasivuni, A comparative review of natural and synthetic biopolymer composite scaffolds, Polymers 13 (7) (2021), https://doi.org/10.3390/polym13071105.

[19] R. Song, M. Murphy, C. Li, K. Ting, C. Soo, Z. Zheng, Current development of biodegradable polymeric materials for biomedical applications (in eng), Drug Des. Dev. Ther. 12 (2018) 3117–3145, https://doi.org/10.2147/DDDT.S165440.

[20] F. Zamboni, S. Vieira, R.L. Reis, J. Miguel Oliveira, M.N. Collins, The potential of hyaluronic acid in immunoprotection and immunomodulation: chemistry, processing and function, Prog. Mater. Sci. 97 (2018) 97–122, https://doi.org/10.1016/j.pmatsci.2018.04.003, 2018/08/01/.

[21] F. Zamboni, et al., On the Bacteriostatic Activity of Hyaluronic Acid Composite Films, 2021.

[22] F. Zamboni, et al., Enhanced cell viability in hyaluronic acid coated poly(lactic-co-glycolic acid) porous scaffolds within microfluidic channels, Int. J. Pharm. 532 (1) (2017) 595–602, https://doi.org/10.1016/j.ijpharm.2017.09.053, 2017/10/30/.

[23] F. Zamboni, et al., Towards the development of a female animal model of T1DM using hyaluronic acid nanocoated cell transplantation: refinements and considerations for future protocols (in eng), Pharmaceutics 13 (11) (2021) 1925, https://doi.org/10.3390/pharmaceutics13111925.

[24] M.N. Collins, C. Birkinshaw, Hyaluronic acid based scaffolds for tissue engineering—a review, Carbohydr. Polym. 92 (2) (2013) 1262–1279, https://doi.org/10.1016/j.carbpol.2012.10.028, 2013/02/15/.

[25] A. Souness, F. Zamboni, G.M. Walker, M.N. Collins, Influence of scaffold design on 3D printed cell constructs, J. Biomed. Mater. Res. B Appl. Biomater. 106 (2) (2018) 533–545, https://doi.org/10.1002/jbm.b.33863, 2018/02/01.

[26] F. Zamboni, E. Ryan, M. Culebras, M.N. Collins, Labile crosslinked hyaluronic acid via urethane formation using bis(β-isocyanatoethyl) disulphide with tuneable physicochemical and immunomodulatory properties, Carbohydr. Polym. 245 (2020) 116501, https://doi.org/10.1016/j.carbpol.2020.116501, 2020/10/01/.

[27] G. Tripodo, A. Trapani, M.L. Torre, G. Giammona, G. Trapani, D. Mandracchia, Hyaluronic acid and its derivatives in drug delivery and imaging: recent advances and challenges, Eur. J. Pharm. Biopharm. 97 (2015) 400–416, https://doi.org/10.1016/j.ejpb.2015.03.032, 2015/11/01/.

[28] C.B. Highley, G.D. Prestwich, J.A. Burdick, Recent advances in hyaluronic acid hydrogels for biomedical applications, Curr. Opin. Biotechnol. 40 (2016) 35–40, https://doi.org/10.1016/j.copbio.2016.02.008, 2016/08/01/.

[29] S. Wang, et al., Fabrication and characterization of conductive poly (3,4-ethylenedioxythiophene) doped with hyaluronic acid/poly (l-lactic acid) composite film for biomedical application, J. Biosci. Bioeng. 123 (1) (2017) 116–125, https://doi.org/10.1016/j.jbiosc.2016.07.010, 2017/01/01/.

[30] M. Culebras, et al., Conducting PEDOT nanoparticles: controlling colloidal stability and electrical properties, J. Phys. Chem. C 122 (33) (2018) 19197–19203, https://doi.org/10.1021/acs.jpcc.8b04981, 2018/08/23.

[31] M.H. Jeong, et al., Increasing the thermoelectric power factor of solvent-treated PEDOT:PSS thin films on PDMS by stretching, J. Mater. Chem. 6 (32) (2018) 15621–15629, https://doi.org/10.1039/C8TA03606C.

[32] D. Alemu, H.-Y. Wei, K.-C. Ho, C.-W. Chu, Highly conductive PEDOT:PSS electrode by simple film treatment with methanol for ITO-free polymer solar cells, Energy Environ. Sci. 5 (11) (2012) 9662–9671, https://doi.org/10.1039/C2EE22595F.

[33] J.Y. Kim, J.H. Jung, D.E. Lee, J. Joo, Enhancement of electrical conductivity of poly(3,4-ethylenedioxythiophene)/poly(4-styrenesulfonate) by a change of solvents, Synth. Met. 126 (2) (2002) 311–316, https://doi.org/10.1016/S0379-6779(01)00576-8, 2002/02/14/.

[34] Z. Yu, Y. Xia, D. Du, J. Ouyang, PEDOT:PSS films with metallic conductivity through a treatment with common organic solutions of organic salts and their application as a transparent electrode of polymer solar cells, ACS Appl. Mater. Interfaces 8 (18) (2016) 11629–11638, https://doi.org/10.1021/acsami.6b00317, 2016/05/11.

[35] W. Jeong, et al., Enhancing the conductivity of PEDOT:PSS films for biomedical applications via hydrothermal treatment, Biosens. Bioelectron. 171 (2021) 112717, https://doi.org/10.1016/j.bios.2020.112717, 2021/01/01/.

[36] J. Shen, Y. Lu, Y. Xu, L. Hou, Biocompatibility of an injectable gel composed of modified hyaluronic acid and adipose-derived mesenchymal cells, Int. J. Clin. Exp. Med. vol. 9 (2016) 19567–19573, 10/30.

[37] I.S. Bayer, Hyaluronic acid and controlled release: a review (in eng), Molecules (Basel, Switzerland) 25 (11) (2020) 2649, 10.3390/molecules25112649.

Further reading

[38] Fernanda Zamboni, C.K. Wong, Maurice Collins N, Hyaluronic acid association with bacterial, fungal and viral infections: Can hyaluronic acid be used as an antimicrobial polymer for biomedical and pharmaceutical applications?458-473, Bioactive Materials 19, (2023) 458–473, https://doi.org/10.1016/j.bioactmat.2022.04.023. In this issue.